EXPERIMENTAL AND NUMERICAL INVESTIGATION OF WOOD DRYING PROCESS USING MODIFIED INFRA-RED HEATING TREATMENT

Erzsébet Cserta, Department of Metallurgy, Chair of Thermal Processing Technology, University of Leoben, Leoben, Austria
Dr. László Könözsy, Department of Metallurgy, Chair for Simulation and Modelling of Metallurgical Processes, University of Leoben, Leoben, Austria
Gergely Hegedűs, Kentech Ltd., Hungary
Prof. Harald Raupenstrauch, Department of Metallurgy, Chair of Thermal Processing Technology, University of Leoben, Leoben, Austria

Introduction

The wood plays an important role as a natural material in the industry. For the engineering practice, the selection of the adequate drying method is indispensable to produce high material quality of the product. Depending on the original material structure and the climate conditions, several drying methods are used according to the type of the energy transfer into the sample. The drying process based on the heat radiation became more and more important research field in the past decades. Essentially, all these technologies use electromagnetic waves to heat up the wood [1-6]. The drying of organic raw materials using infra-red (IR) radiation also takes place among these processes as a relatively new technology.

The wood drying process can be defined as a simultaneous heat and moisture transport with local thermodynamic equilibrium at each point within the probe. The process can accuratly be determined by knowing the temperature distribution in time and space. The complex internal structure of the wood causes difficulties in the simulation at microscopic level. Therefore, the most classical models use homogenization [7-9] or space averaging [10] techniques.

The present paper deals with the drying process of spruce wood *(Picea abies)* in a newly developed IR drying furnace according to the patent Nr. PO 700 453. The required frequency field is ensured by heating wires using modificator layers. During the process, the cellulose molecules are depolymerized, therefore, the water can easily exit from the wood. Several wood types were analysed at different drying conditions to determine the optimal heating parameters. The results of spruce wood was chosen to show the efficiency of the technology. The experimental investigation of the process can be found in the first section.

For the better understanding of the proposed IR drying process, a one-dimensional model has been set up to investigate numerically the heat transfer in wood slab. In the second section of this work, the finite difference method has been used to obtain an approximate solution of the temperature profile. The temperature conductivity has been taken into account based on the experimental data system. The numerically predicted results have been compared to temperature measurements and good agreements with experimental data were obtained.

Experimental investigation

Experimental setup

A newly designed IR furnace has been set up to investigate experimentally the drying process. The flow sheet of the system is shown in the Fig. 1.

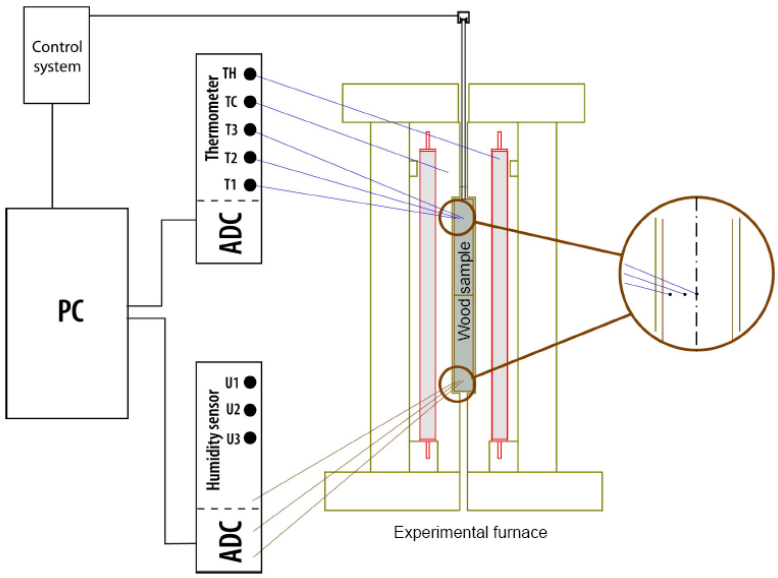

Figure 1. The flow sheet of the experimental set-up; a) the IR furnace; b) the regulation system; c) the data acquisition system.

The test facility consists of the drying furnace with the IR heating system, the data acquisition system and the regulation system. The size of the drying area can be controlled according to the sample size by altering the distance between the heating surfaces. The heating surface is built up of 12 heating wires using modificator layers at the two vertical walls around the sample. The heating power of the wires is completely 4 kW. The infra-red radiation was generated at the wavelength between 700-1000 μm. The regulation system is designed to be eligible both manual and automatic controlling. A digital adquisition system was worked out to store the whole data set. The equipment enables simultaneous measurement of the temperature distribution and moisture content. The temperature was measured using Dixell and Lea K-type thermo-elements. The temperature values appear on the digital screen of the measuring meter and a time-programmed camera is used for recording the data. There were test holes drilled in the drying wood where the sensors of the temperature detectors were located. The moisture content was measured in the test holes as well, and the values were obtained by using Elbez WHT 860 moisture sensors.

Samples

The investigated spruce wood samples were green or air-seasoned timbers. The green ones had an average initial moisture content which was higher than 40%. Therefore, the initial moisture content of the seasoned samples was dependent on the level of the pre-drying process. The final moisture content was under 8% in the overall measurement series. The average initial sample size is a 50 x 100 [mm/mm] cross section. The technological parameters and the physical properties of the spruce samples can be found in Table 1.

Table 1. Technological parateres and physical properties of the spruce samples

Wood sample type	Total heating time [min]	Incubation time [min]	Initinal moisture content [%]	Final moisture content [%]	Average moister loss [%]	Heating wire temperature [°C]
TF7	330	90	45-50	7>	40-42	340
TF8	360	110	42-64	6-25	36-39	300
TF12	1890	1700	44	6-8	37	200
TF11	500	110	18-33	8>	15-25	300
TF105	180	10	18-21	6>	12-15	480

The physical process of wood drying with IR heating treatment

The IR wood drying technology was devided into two parts according to the location of the wood sample. The wood is installed into the drying furnace in the first part of the process, which is the IR furnace drying process. The drying is caused mainly due to heat radiation. The heat transfer occurs due to conduction, when the wood is taken out of the oven. The drying continuous on the free air in the room temperature, in this way, the second part of the process is the post-drying process.

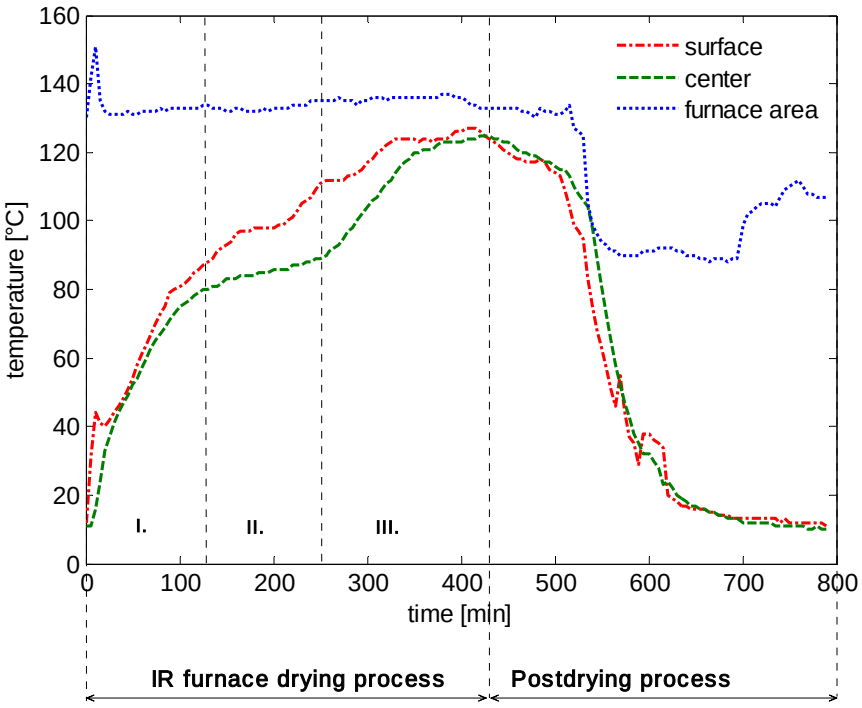

Figure 2. The surface and the center temperature of the TF11 spruce timber depending on time using infra-red radiation, and the average temperature of the furnace area

Three drying periods were determined depending on the temperature distribution in the sample. These are the heating-up etap (I), the incubation etap (II) and the reverse heating etap (III) (see Fig. 2.). The first drying time interval was considered as the heating-up process. The temperature of the sample surface increases faster than the temperature of the wood center. The increment of the core temperature is stopped at around 80 ^{o}C, and the second drying time interval starts at that point. The core temperature profile shows a stagnation in

this significant time interval. When the incubation point is achieved, then an evaporization front startes to move from the surface towards to the center. This phenomenon refers to an internal boiling of the water, and the introduced heat is transformed to latent heat. Corresponding to the low temperature at the stagnation interval, a local suction effect is produced behind the evaporization front. The low pressure is assumed to be the effect of the osmotic mechanism. The semipermeable membrane is built up by cellulose mulecules, which let through only the water molecules. The larger salt molecules are blocked, therefore a concentration difference occurs between the two sides of the cellulosic membrane. The internal osmotic effect is well-balanced by the water-vapor pressure. When the evaporative front reaches the axis of the sample, the core temperature increases faster than the surface temperature. The core temperature can even be higher than the surface temperature. This is an opposite phenomenon compared to the convective drying process. The evaporative front can achive the core, because the cellulose membrane has been depolymerized. The produced temperature gradient helps the moisture content to exit easily, when the core temperature is higher than the surface temperature. When the core temperature reaches or will be above the surface temperature, then the sample will be taken out of the oven. The post-drying process goes further on until the core temperature will be equal to the room temperature.

Brief description of the mathematical model and the numerical solution

A one-dimensional model has been set up to investigate numerically the heat transfer in the wood slab (see Fig. 3.). The finite difference method has been used to obtain an approximate solution of the temperature profile using explicit and implicit schemes. The temperature conductivity, which is one of the most important characteristic of the material, has been taken into account based on the experimental data system. The numerically predicted results have been compared with temperature measurements concerning different process parameters. Considering the complex structural inhomogenity of the wood, it is necessary to have simplifying assumtions. For this reason, the wood is considered as a homogeneous material, the convective heat transport is not taken into account, the moisture content behind the evaporative front is equal to the initial moisture content, and there is local thermal equilibrium inside the material.

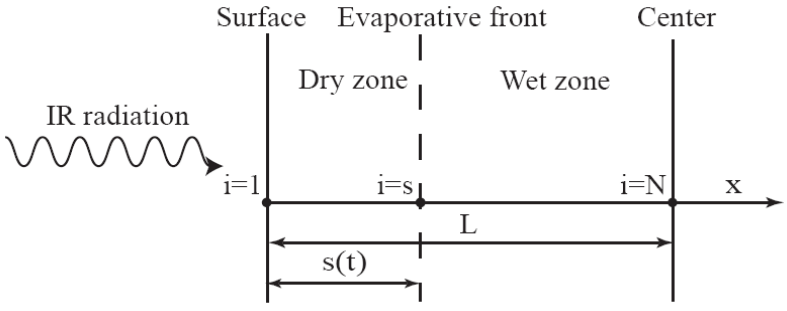

Figure 3. One-dimensional heat conduction model taking into account the movement of the evaporative front during the drying process

The movement of the evaporative front is modelled and it is considered as the moving boundary between the dry and wet part. The Dirichlet boundary conditions at the corners are time-dependent based on the measurements. The radiative term and the latent heat referring to the phase change along the evaporative front is included in the Neumann boundary condition at the moving boundary. The heat conduction equation is solved for both of the dry and wet part of the wood, therefore the governing equation for the dry side of the sample is

$$\frac{\partial \vartheta_1}{\partial t} = \frac{\partial}{\partial x} \cdot \left[\kappa_1(\vartheta_1) \cdot \frac{\partial \vartheta_1}{\partial x} \right], \tag{1}$$

and for the wet side of the sampe is

$$\frac{\partial \vartheta_2}{\partial t} = \frac{\partial}{\partial x} \cdot \left[\kappa_2(\vartheta) \cdot \frac{\partial \vartheta_2}{\partial x} \right], \tag{2}$$

where $\kappa_1(\vartheta_1)$ and $\kappa_2(\vartheta_2)$ are the temperature conductivities of the dry and wet zones of the sample corresponding to ϑ_1 and ϑ_2 temperatures. The temperature dependence of the temparature conductivity for the dry side of the wood is the sum of the conductive term

$$\begin{aligned} \kappa_{cond}(\vartheta_1) = -1.3185 \cdot 10^{-2} + 1.723 \cdot 10^{-7} \vartheta_1 - 1.27 \cdot 10^{-8} \vartheta_1^2 + 7.8071 \cdot 10^{-11} \vartheta_1^3 - \\ - 6.913 \cdot 10^{-13} \vartheta_1^4 + 1.055 \cdot 10^{-14} \vartheta_1^5, \end{aligned} \tag{3}$$

and the radiative term

$$\kappa_{rad}(\vartheta_1) = 17.15 \cdot \varepsilon_{rad} \cdot \sigma \cdot \vartheta_1^3 \cdot d, \tag{4}$$

where ε_{rad} is the radiation emissivity of the wood, σ is the Stefan-Boltzmann constant, and *d* is the equivalent pore diameter [11]. The radiation emissivity can be chosen according to

$$1 \geq \varepsilon_{rad} \geq 0.9. \tag{5}$$

The surrounding air and the wood can be considered magnetically transparent at the modified frequency field. The incident radiation, emitted from the heating wires, reaches the wood and penetrates into the inhomogenouos structure until it is absorbed by the moisture of the wood. Consequently, the most important absorbtion effect is evolved in the evaporative front. This plane of the evaporization is taken into account as an internal wet surface of the wood, where the IR radiation is absorbed. Behind this front, the effect of the radiative heat term can be neglected in the wet zone of the sample. According to Eqs. (3)-(4), the following expression may valid for the temperature conductivity

$$\kappa_1(\vartheta_1) = \kappa_{cond}(\vartheta_1) + \kappa_{rad}(\vartheta_1). \tag{6}$$

The temperature conductivity $\kappa_2(\vartheta_2)$ is considered as a constant in the wet side of the sample. Since, the movement of the evaporative front is computed, therefore it is necessary to specify boundary condition at the moving boundary. Concerning the above mentioned assumptions, the moving boundary condition of the evaporative front can be fullfilled as

$$\alpha_1(\vartheta_1) \cdot \left. \frac{\partial \vartheta_1}{\partial x} \right|_{s(t)} = \alpha_2(\vartheta_2) \cdot \left. \frac{\partial \vartheta_2}{\partial x} \right|_{s(t)} + S_{ph} + S_{rad}, \tag{7}$$

where

$$\begin{aligned} \alpha_1(\vartheta_1) = -9.23 \cdot 10^{-3} + 1.213 \cdot 10^{-7} \vartheta_1 - 8.858 \cdot 10^{-9} \vartheta_1^2 + 5.115 \cdot 10^{-11} \vartheta_1^3 - \\ - 4.839 \cdot 10^{-13} \vartheta_1^4 + 7.386 \cdot 10^{-15} \vartheta_1^5 \end{aligned} \tag{8}$$

is the thermal conductivity of the dry section of the wood, S_{ph} is the latent heat corresponding to the phase change during the evaporization, and S_{rad} is the additional heat term from the radiative heat absorbtion at the evaporative front. The S_{ph} is given according to [12,13] considering the movement of the phase change as a function of time. The value of the S_{rad} is computed from the mean radiation power density locally absorbed by the sample [5,6]. The thermal conductivity $\alpha_2(\vartheta_2)$ is considered as a constant in the model. The parameter values are implemented in the simulation based on the measurements.

The solution of Eqs. (1)-(2) time-dependent and non-linear parabolic heat conductions were obtained by explicit finite difference method. An in-house MATLAB code was implemented to estimate the temperature distribution in the wood slab. The temperature dependence of the temparature conductivity were taken into account based on the Eq. (3) in the dry side of the sample. The choise of the temporal and spacial terms are not arbitrary in the explicit method. It is essential to determine these terms according to the accuracy and stability conditions. The stability of the algorithm has to be ensured, therefore the following formula can be derived for the time-step size to satisfy the stability criterion as

$$\Delta t \leq \frac{(\Delta x)^2}{2\kappa_1(\vartheta_1)}. \tag{9}$$

For solving the one-dimensional non-linear parabolic heat conduction equation, the explicit method is adviced, because it can be easily implemented. For solving the Eqs. (1)-(2) using an implicit method, it is necessary to linearize the right hand side of the equations. The Crank-Nicolson implicit scheme was used. This method computes temperature values between two time-levels. For implicit solution of the one-dimensional heat conduction problem, a tridiagonal system of linear equations has to be solved. The numerically predicted results will be discussed in the next section.

Results and discussion

For reaching the required material quality in the wood industry, the optimal heating parameters is to be determined. The heating rate was altered and adjusted according to the pre-drying level of the samples. These samples were experimentally investigated with different initial moisture content (see Table 1.). The decomposition time of the cellulose during the furnace drying process is strongly determined by the initial stage of the wood. The air-seasoning process has strong effect on the drying. When the cellulosic membrane is already decomposed during this process, afterwards the incubation period is insignificant. An inflection point can only be detected as it is shown in the Fig. 4.c. The initial free moisture content has small influence on the heating time, because the major part of the installed heat is used for the elimination of the chemically bound water (see Fig. 4.b.). After the decomposition of the cellulosic membrane, the moisture can easily exit without causing internal cracks. It is also essential to take care of the internal temperature gradient during the incubation time. When the internal temperature difference is kept under 20 °C degree, the internal crack formation can be avoided. Above this temperature gradient value, the cells may be exploded and internal cracks might be formed in the slab (see Fig. 4.d.). It is important to find the optimal heating rate, because the core temperature can reach the surface temperature only in that case, when the radiation intensity is high enough (see Fig. 4.a.).

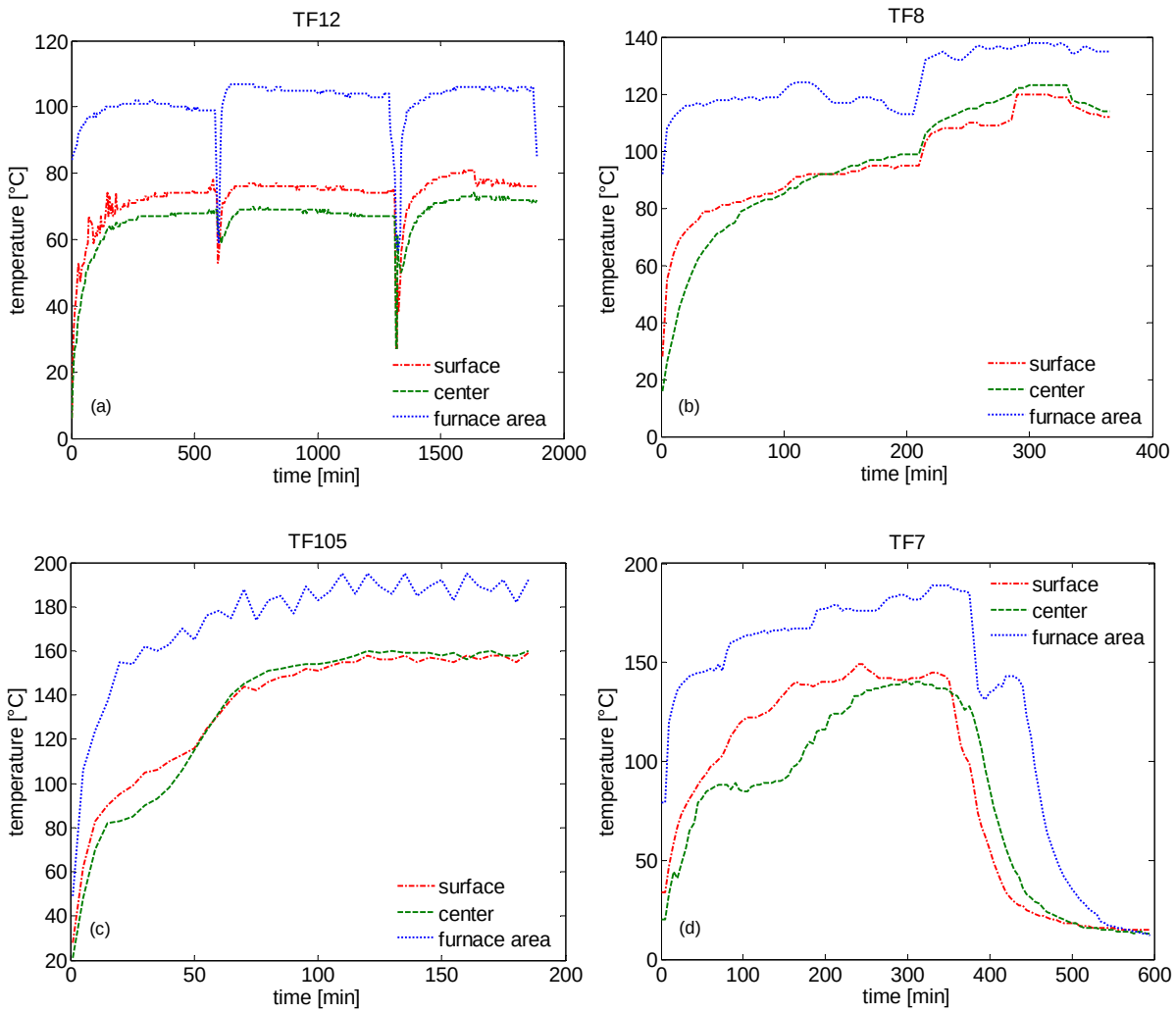

Figure 4. The surface and the center temperature of green (a, b, d) and seasoned (c) spruce timbers depending on time, and the average temperature of the furnace area

The measured temperature curves in the Fig. 4.a-d. give the boundary values for the mathematical model. The temperature were measured at the surface, the core and the mid-point of the computational domain. In this way, it was possible to test the model using time-dependent boundary conditions. The measurements data were implemeted, and the aim of the numerical investigation was to analyse how the computed curves approch the measured points. The computed curves in the domain were displayed in every 20^{th} minutes (see Fig. 5 and Fig. 6.). The predicted results were compared to the experimental data. It means that the mathematical model can reproduce the measured temperature distribution. The simulation curves fit to the measured point (see Fig 5.a-b). Although, differences can be observed at higher temperatures, the tendency of the temperature values are still similar. Using the temperature dependent conductivity, an acceptable agreement can be achived with the experimental data.

The movement of the evaporative front is shown in the Fig. 6.a-b. The location of the evaporative front is indicated by circles. The characteristic of this moving front shows exponential behaviour. It agrees with our assumptions that the evaporation process recedes towards to the center, which is caused by the absorptive power of the water. The radiative term was neglected in the wet zone, because the moisture content absorbs the main part of the

radiation entering in the wood. The influance of the radiation effect has importance in the dry zone, where the moisture content is not continuous in reality.

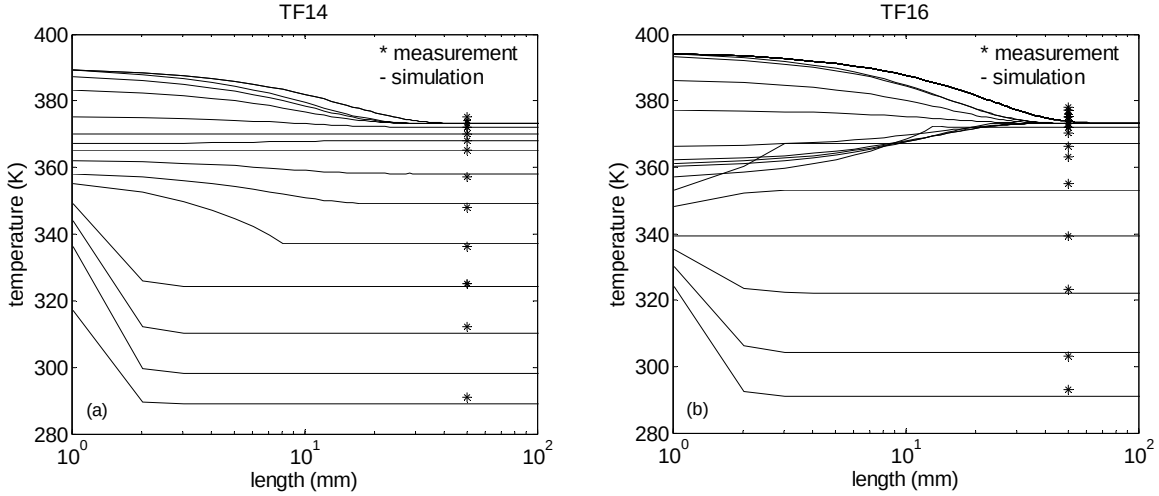

Figure 5. Comparison of the simulated and measured temperature field in the mid-point of the spruce wood in the computational domain

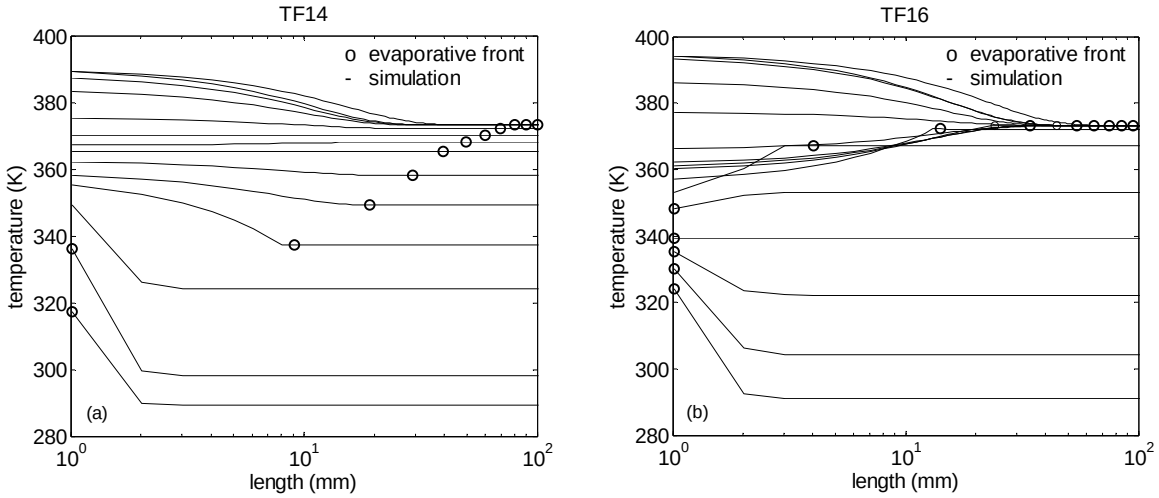

Figure 6. The simulated temperature distribution and the receding evaporative front in the computational domain

Conclusion

The present paper deals with the drying process of spruce wood in a newly developed IR drying furnace according to the patent Nr. PO 700 453. The required frequency field is ensured by heating wires using modificator layers at the optimal heating rate. The IR drying process is developed to have an effective time and energy save technology. A one-dimensional model was set up to investigate numerically the heat transfer in the wood slab. The finite difference method was used to obtain an approximate solution of the temperature profile using explicit and implicit schemes. The numerically predicted results were compared to temperature measurements concerning different process parameters. An acceptably good agreement with experimental data were obtained. For the future work, it is essential to take into account that the optimal heating rate is strongly depending on the inhomogeneous structure of the wood. This research can be a basis of the investigation of further woods.

Acknowledgements

This work is financially supported by the Kotla-Project for which the authors kindly acknowledge. The authors wish to express their appreciation to Sedo Group Ltd., Askada Ltd., and Kentech Ltd. for their industrial contribution in the experimental work as well.

References

1. Rattanedecho, P. (2006), "The Simulation of Microwave Heating of Wood Using a Rectangularwave Guide-Influence of Frequency and Sample Size," *Chemical Engineering Science*, March, pp. 4798-4811.
2. Haghi, A. K. and Ghandzadeh, H. (2006), "Experimental study on combined inrfared and microwave drying of porous media with particular application in wood industry," *Int. J. of Applied Mechanics and Engineering*, Vol. 11, pp. 985-991.
3. Oloyede, A. and Groombridge P. (2000), "The Influence of Microwave Heating on the Mechanical Properties of Wood," *Journal of Materials Processing Technology*, August, pp. 67-73.
4. Hansson L. and Antti A.L. (2002), "The effect of microwave drying on Norway spruce woods strength: a comparison with conventional drying," *Journal of Materials Processing Technology*, November, pp. 41-50.
5. Turner, I. W. and Perré, P. (2004), "Vacuum drying of wood with radiative heating: II. Comparison between theory and experiment," *AIChE Journal***,** Vol. 50, pp. 108-118.
6. Bucki, M. and Perré, P. (2003), "Radio requency/vacuum drying of wood: A comprihensive 2-D computational model on the board's scale," *8th International IUFRO Wood Drying Conference*, pp. 33-38.
7. Awadalla, H.S.F. and El-Dib, A.F. and Mohamad, M.A. and Reuss M. and Hussein. H.M.S. (2004), "Mathematical modelling and experimental verification of wood drying process," *Energy Conversion and Management*, pp. 197-207.
8. Shusheng, P. and Keey, R. B. (1995), "Modelling the temperature profiles within board during the high-temperature drying of Pinus radiata timber: the influence of airflow reversals," *Int. J. Heat Mass Transfer*, pp. 189-205.
9. Surasani, V.K. and Metzger, T. and Tsotsas E. (2008), "Consideration of heat transfer in pore network modelling of convective drying," *International Journal of Heat and Mass Transfer*, Vol. 51, pp. 2506-2518.
10. Erriguible, A. and Bernada, P. and Couture, F. and Roques, M.-A. (2007), "Simulation of vacuum drying by coupling models," *Chemical Engineering and Processing*, Vol. 46, pp. 1274-1285.
11. Thunman, H. and Lecker, B. (2002), "Thermal conductivity of wood – models for different stages of combustion," *Biomass and Bioenergy*, Vol. 23, pp. 47-54.
12. Czibere, T. (1998), "Vezetéses hőátvitel (in Hungarian)," Miskolc University Press
13. Forest Products Laboratory (2002), "Wood Handbook – Wood as an engineering material," *USDA Forest Service*, Madison, Wisconsin